Rhythm Dynamics of the Aging Heart: an Experimental Study Using Conscious, Restrained Mice

Martina Comelli, Marianna Meo, Daniel O Cervantes, Emanuele Pizzo, Aaron Plosker, Peter J Mohler, Thomas J Hund, Jason T Jacobson, Olivier Meste, Marcello Rota

Am J Physiol Heart Circ Physiol 319: H893–H905, 2020.
First published September 4, 2020; doi:10.1152/ajpheart.00379.2020.

RESEARCH ARTICLE | *Integrative Cardiovascular Physiology and Pathophysiology*

Rhythm dynamics of the aging heart: an experimental study using conscious, restrained mice

Martina Comelli,[1] Marianna Meo,[2] Daniel O. Cervantes,[1] Emanuele Pizzo,[1] Aaron Plosker,[1] Peter J. Mohler,[3,4,5] Thomas J. Hund,[3,5,6] Jason T. Jacobson,[1,7] Olivier Meste,[8] and Marcello Rota[1]

[1]*Department of Physiology, New York Medical College, Valhalla, New York;* [2]*IHU Liryc, Electrophysiology and Heart Modeling Institute, Bordeaux University Foundation, F-33600 Pessac-Bordeaux, France, with Univ. Bordeaux and INSERM, CRCTB, U1045, Bordeaux, France;* [3]*The Frick Center for Heart Failure and Arrhythmia, Dorothy M. Davis Heart and Lung Research Institute, The Ohio State University Wexner Medical Center, Columbus, Ohio;* [4]*Department of Physiology and Cell Biology, The Ohio State University College of Medicine, Columbus, Ohio;* [5]*Department of Internal Medicine, The Ohio State University College of Medicine, Columbus, Ohio;* [6]*Department of Biomedical Engineering, College of Engineering, The Ohio State University, Columbus, Ohio;* [7]*Division of Cardiology, Department of Medicine, Westchester Medical Center, New York Medical College, Valhalla, New York; and* [8]*Laboratoire d'Informatique, Signaux et Systèmes de Sophia Antipolis, Université Côte d'Azur, CNRS, I3S, France*

Submitted 18 May 2020; accepted in final form 29 August 2020

Comelli M, Meo M, Cervantes DO, Pizzo E, Plosker A, Mohler PJ, Hund TJ, Jacobson JT, Meste O, Rota M. Rhythm dynamics of the aging heart: an experimental study using conscious, restrained mice. *Am J Physiol Heart Circ Physiol* 319: H893–H905, 2020. First published September 4, 2020; doi:10.1152/ajpheart.00379.2020.—Heart rate variability (HRV) is a measure of variation in time interval between heartbeats and reflects the influence of autonomic nervous system and circulating/locally released factors on sinoatrial node discharge. Here, we tested whether electrocardiograms (ECGs) obtained in conscious, restrained mice, a condition that affects sympathovagal balance, reveal alterations of heart rhythm dynamics with aging. Moreover, based on emergence of sodium channels as modulators of pacemaker activity, we addressed consequences of altered sodium channels on heart rhythm. C57Bl/6 mice and mice with enhanced late sodium current due to Nav1.5 mutation at Ser571 (S571E) at ~4 to ~24 mo of age, were studied. HRV was assessed using time- and frequency-domain and nonlinear parameters. For C57Bl/6 and S571E mice, standard deviation of RR intervals (SDRR), total power of RR interval variation, and nonlinear standard deviation 2 (SD2) were maximal at ~4 mo and decreased at ~18 and ~24 mo, together with attenuation of indexes of sympathovagal balance. Modulation of sympathetic and/or parasympathetic divisions revealed attenuation of autonomic tone at ~24 mo. At ~4 mo, S571E mice presented lower heart rate and higher SDRR, total power, and SD2 with respect to C57Bl/6, properties reversed by late sodium current inhibition. At ~24 mo, heart rate decreased in C57Bl/6 but increased in S571E, a condition preserved after autonomic blockade. Collectively, our data indicate that aging is associated with reduced HRV. Moreover, sodium channel function conditions heart rate and its age-related adaptations, but does not interfere with HRV decline occurring with age.

NEW & NOTEWORTHY We have investigated age-associated alterations of heart rate properties in mice using conscious electrocardiographic recordings. Our findings support the notion that aging is coupled with altered sympathovagal balance with consequences on heart rate variability. Moreover, by using a genetically engineered mouse line, we provide evidence that sodium channels modulate heart rate and its age-related adaptations.

Correspondence: M. Rota (marcello_rota@nymc.edu).

aging; heart rate variability; sodium current; sympathovagal balance

INTRODUCTION

Heart rate variability (HRV) is the physiological phenomenon of variation of the interval between heartbeats, which is accounted by the influence of external factors on the pacemaker activity of the heart. The ability of the heart to adjust beating rate is an important mechanism of regulation of cardiac output, allowing the organ to meet hemodynamic requirements under various conditions.

The automaticity of the sinoatrial node (SAN) is based on the combination of transmembrane ionic fluxes (voltage clock) and intracellular calcium release mechanisms (calcium clock), resulting in the progressive depolarization of SAN cells and attainment of the threshold for the upstroke of the action potential (25). Transmembrane ionic currents involved in the process include potassium current, the funny current I_f, calcium currents, and the electrogenic current generated by Na^+/Ca^{2+} exchange (25). Interestingly, sodium channels have emerged as key components of discharge and conduction of the SAN (27, 29), but the precise contribution of these proteins to pacemaker process remains to be validated and clarified.

The SAN is largely under the influence of catecholamines and acetylcholine released by the autonomic nervous system (34). Catecholamines bind β-adrenergic receptors leading to activation of adenylyl cyclase and downstream effectors, which interact with components of the voltage and calcium clocks resulting in faster SAN discharge (34). In contrast, acetylcholine stimulates muscarinic receptors leading to, in a dose-response manner (33), inhibition of adenylyl cyclase and then activation of G protein-regulated channels originating I_{KACh}, an outward current that opposes diastolic depolarization and reduces heart rate (33, 34). Because of the direct effect of acetylcholine on I_{KACh}, consequences of parasympathetic activation on the SAN are almost instantaneous, with latency less than 500 ms (1, 43). Moreover, the high level of acetylcholin-

esterase in the SAN renders effects of vagal impulse brief. In contrast, β-adrenergic receptor stimulation has longer latency effects on the SAN (up to 5 s) (1, 43). Thus, these responses affect the modality of heart rhythm dynamics.

Aging is the major independent risk factor of chronic heart failure and the leading cause of death in people ≥65 yr of age (8). Clinical studies have revealed that aging is associated with reduction of HRV (5, 59, 62), possibly as a consequence of decreased autonomic modulation. However, the precise mechanisms underlying the attenuated HRV with advancing age remain to be documented. Moreover, aging is coupled with reduced maximal heart rate (45), which impacts on maximum rate of oxygen consumption and exercise capacity. Decreased maximal heart rate with aging is correlated to attenuated intrinsic heart rate (13), pointing to defective SAN function as a determinant of the limited adaptability of the aged heart.

In the current study, we have implemented a methodology comprising collection of electrocardiograms (ECGs) in conscious, restrained aging mice, pharmacological interventions modulating sympathetic and/or parasympathetic arms of the autonomic nervous systems, and analysis of heart rhythm dynamics, in the attempt to define intrinsic and extrinsic factors contributing to adaptations intervening in the aged heart. Our acquisition protocol resulted in rapid heart rate in mice, an indication of sympathetic activation in response to stress related to forced immobilization, imposing caution in data interpretation. Overall, our findings support the notion that aging is coupled with altered balance of sympathetic and vagal inputs with consequences on HRV. Moreover, by using a genetically engineered mouse line, we provide evidence that sodium channels modulate heart rate and its age-related adaptations.

METHODS

Animals. Mice were maintained in accordance with the *Guide for Care and Use of Laboratory Animals*, and animal experiments were approved by the local *Institutional Animal Care and Use Committee*. Male C57Bl/6 mice were obtained from Charles River and National Institute of Aging rodent colony. Age-matched genetically engineered male mice with phosphomimetic mutation of sodium channel Nav1.5 at Ser571 (S571E) were obtained from the laboratory of Drs. Hund and Mohler and maintained in our facility. Knockin mice were generated in C57Bl/6 background (18).

Electrocardiographic recording in the conscious state. To record electrocardiograms (ECGs) in conscious animals, an ECG-tunnel device (Emka Technologies) was employed (15, 41). Animals were placed in a tunnel and ECGs recorded for a period of 10 min. Electrical signals were amplified with a 12 Lead ECG Amplifier (DSI, Ponemah), digitized using a 160 kHz A/D converter (DI-1120 HS, Dataq) and recorded with WinDaq software (Dataq). The bipolar lead I, II, and III and the unipolar lead aVL were collected. Electrical signals were evaluated offline.

Drugs. Effects of pharmacological compounds on heart rate and HRV were tested by comparing 10-min ECG recordings obtained before and after drug administration. In between acquisitions, mice were returned to their cages.

To interfere with autonomic nervous system, mice were administered with atropine (0.5 mg/kg body wt ip; Sigma-Aldrich,) for parasympathetic blockade, propranolol (1 mg/kg body wt ip; Sigma-Aldrich) for sympathetic blockade, or the combination of atropine (0.5 mg/kg body wt ip) plus propranolol (1 mg/kg body wt ip) for combined block of sympathetic and parasympathetic branches of the autonomic nervous system (combined autonomic block). Drugs were dissolved in USP saline solution. Effects of parasympathetic, sympathetic, or combined autonomic block were evaluated ~10 min after drug administration. Timing of acquisition and dosages of atropine and propranolol are similar to those used in mice by other groups (9, 14, 17, 28, 38, 47, 60).

To inhibit the late sodium current (I_{NaL}) mice received GS967 (0.5 mg/kg body wt ip; Apexbio) (3, 56a) dissolved in USP saline solution. Following baseline acquisition, effects of GS967 were tested at ~30 min after drug administration. Time course tests confirmed that effects of GS697 administration on RR interval duration were comparable at 10, 30, and 60 min after drug injection (Fig. S1 in the Supplemental Data, https://doi.org/10.6084/m9.figshare.12648872.v1).

Settings for data analysis. Analysis of heart rate and HRV was conducted on electrocardiographic recordings using LabChart 8 (ADinstruments) and the heart variability (HRV) module (see Supplemental Data). Lead I was used to obtain HRV parameters, and other leads were employed as alternative source of analysis and/or for validation of obtained results. The entire 10-min recording was assessed. Company presets of LabChart HRV module for the mouse were adopted, with minor modifications of parameters for beat classification. Specifically, valid RR intervals were included in the range 70–120 ms and complexity in the range 0.5–1.5. Recordings with less than 1,000 detected beat over the 10 min of acquisition were excluded from the analysis. A report providing parameters of HRV was generated by the software and values exported to Microsoft Excel for quantification. Moreover, part of the data was tested with a customized algorithm for HRV assessment (see Supplemental Data).

Parameters employed to describe heart rate and HRV. The RR interval duration was quantified by the average of RR intervals (average RR) obtained during the 10 min of acquisition. HRV was quantified by using the following (1, 17, 43, 60). First, time-domain variables were standard deviation of RR intervals (SDRR); coefficient of variation of RR intervals (CVRR), obtained by dividing SDRR by average RR interval; and square root of the mean of the squared differences between adjacent RR intervals (RMSSD), an index of short-term variability. Second, frequency-domain variables were total power (ms^2), corresponding to energy in the entire power spectrum analyzed (0–5 Hz); very low-frequency power (VLF, ms^2), corresponding to energy in the power spectrum between 0 and 0.15 Hz; low-frequency power (LF, ms^2), corresponding to energy in the power spectrum between 0.15 and 1.5 Hz; and high-frequency power (HF, ms^2), corresponding to energy in the power spectrum between 1.5 and 5 Hz. Data for VLF, LF, and HF were also computed as percentage of the total power (%). Moreover, low-frequency/high-frequency ratio (LF/HF, ms^2/ms^2), the ratio of low-frequency to high-frequency power, is reported. High-frequency components of RR interval variations reflect respiratory-mediated modulation of heart rate by the parasympathetic system, whereas low-frequency components reflect baroreflex-mediated modulation of heart rate (43, 48). Very low-frequency components of RR interval variation reflect the influence of the renin-angiotensin system, thermoregulation, and, in part, parasympathetic activity (48). Overall, the very low-frequency band appears to be a parameter that most closely informs on intrinsic sinoatrial node components of HRV versus autonomic input components. The significance of low-frequency components is not fully agreed upon, but it is generally accepted that it is influenced by both the sympathetic and parasympathetic system (43). Importantly, the LF/HF ratio is considered a parameter for the assessment of sympathovagal balance, estimating the ratio of sympathetic to vagus nerve tone (1, 43), although this concept has been challenged based on the fact that low-frequency components of RR interval variability are affected by sympathetic, parasympathetic, and other unidentified factors (10). Third, nonlinear parameters were indexes obtained from the Poincaré plot, a scatter graph obtained by plotting each RR interval (RR_n) against the next one (RR_{n+1}) (16, 46). By an ellipse-fitting technique of plotted data, the following indexes were obtained: standard deviation of instantaneous beat-to-beat interval variability (SD1), standard deviation of continuous long-term RR interval variability (SD2), and SD1/SD2

ratio. SD1 correlates with the short-term variability of heart rate and is mainly influenced by parasympathetic modulation. In contrast, SD2 is a measure of long-term variability and reflects sympathetic activation (46). The ratio SD1/SD2 is an index of autonomic balance, and it correlates with the LF/HF ratio (48).

Surface ECG intervals were measured using LabChart 8. To reduce electrical noise and motion artifacts, ~25 consecutive beats were averaged by the software and employed to calculate heart rate and electrocardiographic parameters. QRS duration and QT interval were measured by determining the earliest onset and latest offset of ventricular deflections from the averaged cycles. Rate-corrected QT interval (QTc) was calculated using the Bazett formula ($QTc = QT/\sqrt{RR}$) (37, 52, 54).

Data analysis. Data are presented in the text as means ± SD and graphically as medians and interquartile ranges, unless otherwise specified. Statistical analysis was performed using SigmaPlot 11.0 and GraphPad Prism. Data were initially tested for normality (Shapiro-Wilk) and equal variance for assignment to parametric or nonparametric analysis. Parametric tests included Student's *t*-test or analysis of variance followed by Bonferroni test for nonpaired comparison between two or among multiple groups, respectively. For paired statistical analysis, paired *t* test was employed. When normality or equal variance were not met, analysis was performed using Mann–Whitney Rank sum test or Kruskal–Wallis one-way analysis of variance on ranks followed by Dunn's method, for nonpaired comparison between two or among multiple groups, respectively. Wilcoxon signed rank test was employed for paired comparison (12, 36, 37, 52, 54, 55). χ^2-test for trend, Pearson and Spearman correlation tests, and survival curve comparison with Gehan–Breslow–Wilcoxon and log-rank (Mantel–Cox) tests were performed using GraphPad Prism software. $P < 0.05$ was considered significant. Graphs were prepared using GraphPad Prism.

RESULTS

Effects of aging on heart rate and HRV. To evaluate the effects of aging on heart rhythm, male C57Bl/6 mice at 3–5 (~4 mo), 12–13 (~12 mo), 17–19 (~18 mo), and 23–25 (~24 mo) mo of age were studied over a period of 10 min using electrocardiographic recordings in the conscious state, with the animal restrained in a tunnel device equipped with electrodes (41). For the entire group of aging animals, heart rate (724 ± 30 beats/min) was substantially higher with respect to previous observations in aging mice using nonrestrained telemetric assessments (52), an indication of sympathetic activation in response to physical and emotional stress associated by forced immobilization (24).

Average RR interval duration was preserved from ~4 to ~18 mo, but increased at ~24 mo, by ~4% (Fig. 1, *A* and *B*). By time-domain variable analysis, standard deviation of RR intervals (SDRR), and coefficient of variance of RR intervals (CVRR) were maximal at ~4 mo and decreased at older age, with reduction of ~25% in mice at ~24 mo (Fig. 1*C*). In contrast, the short-term variability index RMSSD was preserved at various time points.

By frequency-domain analysis, total power, and very low-frequency and low-frequency components of RR interval variations were maximal at ~4 mo and decreased thereafter, whereas high-frequency components were comparable for animals at different ages (Fig. 1*D*). When normalized with respect to total power, very low- and low-frequency components were reduced with age, whereas normalized high-frequency components progressively increased and reached a maximum at ~24 mo (Fig. 1*E*). The LF/HF ratio, which is generally accepted as an index of sympathovagal balance (1, 43), was maximal at ~4 mo and significantly decreased at ~18 and ~24 mo (Fig. 1*F*).

By Poincaré plots, clusters of data points for young and old mice appeared differently distributed, based on dissimilarities of RR interval duration and its variability (Fig. 1*G*). Quantitatively, beat-to-beat interval variability (SD1) was comparable at various age intervals, whereas standard deviation of continuous long-term RR interval variability (SD2) was maximal at ~4 mo and decreased thereafter (Fig. 1*H*). As a consequence, SD1/SD2, an index of vagal and sympathetic balance (48), was minimal at ~4 mo and significantly increased at ~18 and ~24 mo.

To test reproducibility of results obtained with the commercially available software LabChart, a previously employed customized ECG processing algorithm (11) adapted for mouse ECG was used (Fig. S2 and S3 in the Supplemental Data). The two analytical platforms differed in settings and methodology of beat detection, processing of input RR interval series, and use of segmented analysis. Despite these differences, results originated from the two analytical systems were overall comparable in reporting age-related decline of HRV in C57Bl/6 mice (Fig. S4 and S5 in the Supplemental Data).

Therefore, under our experimental conditions, aging in mice is coupled with reduction of heart rate, decline of HRV, and altered indexes of sympathovagal balance.

Aging and modulation of heart rate by autonomic nerve activity. To define the contribution of autonomic nervous system on heart rate and its variability observed with our acquisition protocol, electrocardiographic recordings in the conscious state were obtained in male mice at 3–4 mo of age (young) and mice at 24–27 mo (old) at baseline and after administration of propranolol and atropine to achieve combined autonomic blockade (17, 37, 38, 52). As reported in Table S1 in the Supplemental Data and summarized in Fig. 2*A*, combined autonomic block increased average RR interval duration in young (10 ± 5%) and old mice (16 ± 8%), exacerbating the difference of RR interval duration between the two groups of animals observed under baseline condition. Combined autonomic block reduced SDRR in young animals by 18 ± 44% but had no effects on SDRR in old mice, leading to attenuation of differences observed for the two groups of mice under baseline condition. Additionally, beat-to-beat variability evaluated by RMSDD was not affected by combined administration of the two drugs.

By frequency-domain analysis, combined autonomic block did not significantly alter low-frequency and high-frequency components of RR interval variations in the two groups of animals, but very low-frequency components were reduced in young mice by 36 ± 80%. Moreover, normalized very low- and low-frequency bands were significantly attenuated in young mice after administration of the two blockers, whereas the normalized high-frequency band was enhanced, resulting in decreased LF/HF ratio (Table S1 in the Supplemental Data). These effects were not observed in old animals.

By nonlinear analysis (see Fig S6 and Table S1 in the Supplemental Data), beat-to-beat interval variability (SD1) was not affected in young and old mice after autonomic blockade. In contrast, only in young animals, long-term RR interval variability (SD2) decreased, whereas SD1/SD2 increased. Changes induced by combined autonomic block ab-

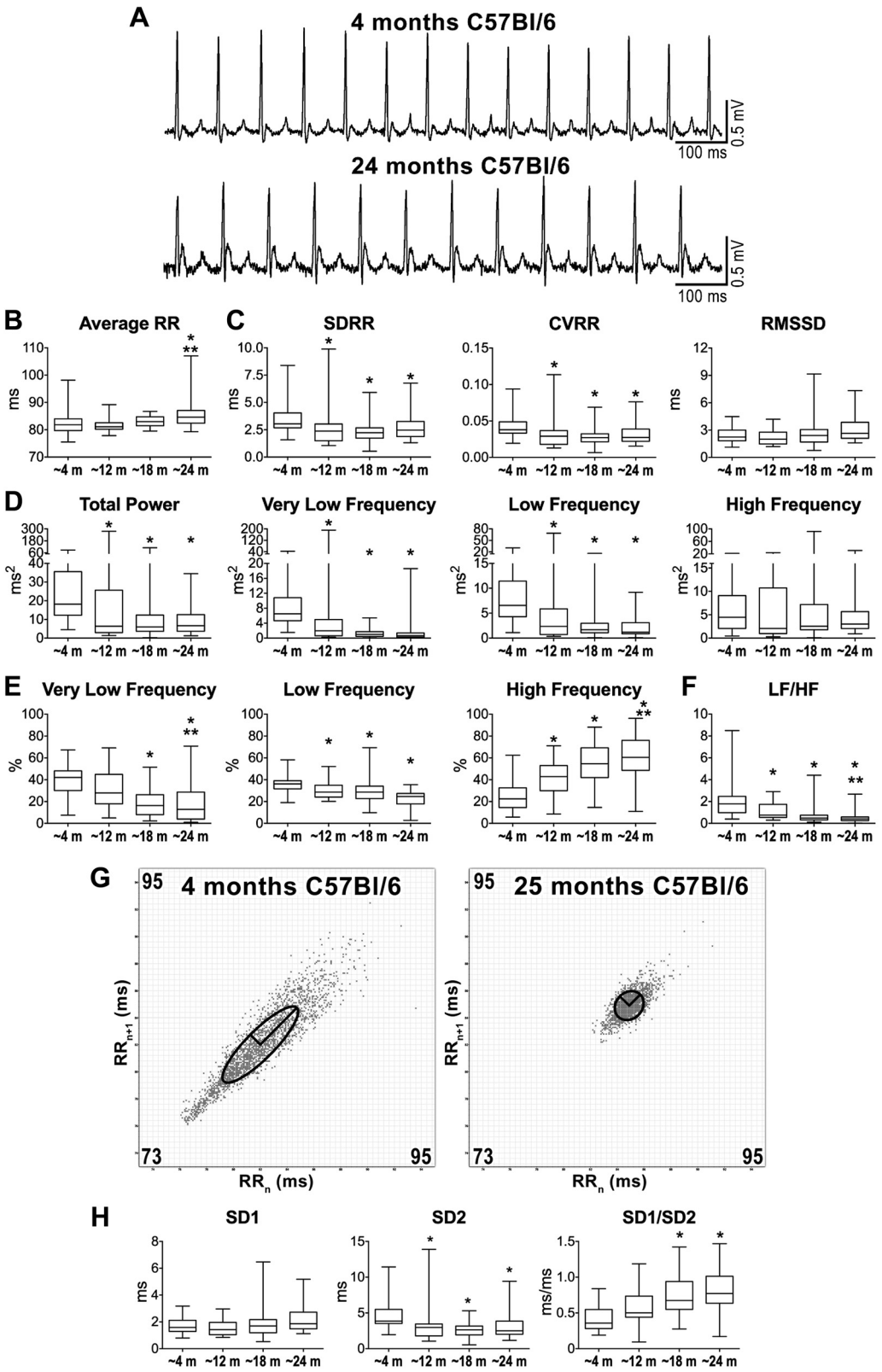

Fig. 1. Aging and alterations of heart rate properties. *A*: ECGs recorded in C57Bl/6 male mice at 4 and 24 mo of age. *B*: data for average RR interval duration. *C*: data for time-domain parameters of heart rate variability (HRV). SDRR, standard deviation (SD) of RR intervals; CVRR, coefficient of variation of RR intervals; RMSSD, square root of the mean of the squared differences between adjacent RR; m, months. *D*: frequency-domain parameters of HRV for aging mice. *E*: frequency bands normalized by total power. *F*: data for low frequency-to-high frequency (LF/HF) ratio. *G*: Poincaré plots obtained from ECGs recorded from male C57Bl/6 mice at 4 and 25 mo of age. RR_n and RR_{n+1} axes span from 73 to 95 ms. *H*: data for nonlinear indexes. Quantitative data shown in *B–F* and *H* were obtained from mice at ~4 mo ($n = 44$), ~12 mo ($n = 23$), ~18 mo ($n = 31$), and ~24 mo ($n = 30$) of age. Data are presented as medians and interquartile ranges. *$P < 0.05$ vs. ~4 mo. **$P < 0.05$ vs. ~12 mo.

rogated differences between the two groups of mice observed under baseline condition.

Thus, autonomic block prolongs RR interval in young and old mice but reduces HRV exclusively in young animals, attenuating age-related differences observed with intact autonomic nervous tone. The persistence of prolonged RR interval duration in old mice following combined autonomic block suggests that alterations of intrinsic mechanisms of pacemaker

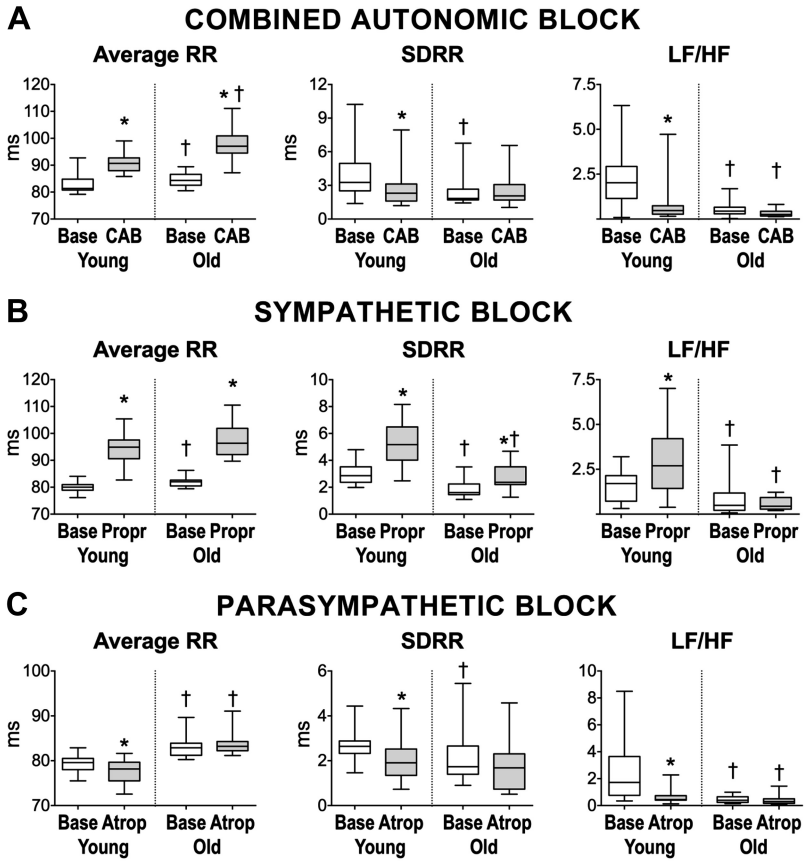

Fig. 2. Effects of modulation of the autonomic nervous system on heart rate properties of aging mice. *A*: data for average RR interval duration, standard deviation of RR intervals (SDRR), and low frequency-to-high frequency (LF/HF) ratio in mice at 3–4 mo of age (young, $n = 20$) and mice at 24–27 mo of age (old, $n = 17$) before (base) and after combined autonomic block (CAB). *B*: data for average RR interval duration, SDRR, and LF/HF ratio in C57Bl/6 mice at 5–6 mo (young, $n = 14$) and mice at 25 mo (old, $n = 11$) before (base) and after propranolol (Propr) administration. *C*: data for average RR interval duration, SDRR, and LF/HF ratio in C57Bl/6 mice at 4–6 mo (young, $n = 21$) and at 20–25 mo (old, $n = 13$) before (base) and after atropine (Atrop) administration. Data are presented as medians and interquartile ranges. *$P < 0.05$ vs. baseline; †$P < 0.05$ vs. young under same experimental condition.

function are responsible for the lower heart rate in aged mice, whereas autonomic modulation tends to attenuate these defects. Additionally, the lack of major changes in HRV following autonomic block in old mice seems to suggest that the modulatory actions of the two arms of the autonomic nervous system are attenuated in old mice with respect to young animals.

Aging and modulation of heart rate by the balance of sympathetic and parasympathetic arms. To better define the contribution of sympathetic and parasympathetic nerve activity on HRV, young male mice at 4–6 mo of age (young) and male mice at 20–25 mo of age (old) were treated with either propranolol or atropine. As reported in Table S2 in the Supplemental Data and summarized in Fig. 2*B*, sympathetic blockade with propranolol alone (17) increased average RR interval duration by 18 ± 6% in young mice and by 19 ± 6% in old. Importantly, sympathetic blockade abrogated differences of RR interval duration between young and old mice observed at baseline. Moreover, propranolol increased SDRR in young and old animals by 79 ± 52% and 67 ± 70%, respectively, whereas RMSDD was enhanced exclusively in young mice by 40 ± 38%.

Sympathetic blockade in young animals enhanced total power and all components of RR variability, together with the LF/HF ratio, whereas this effect was not observed in old mice. Importantly, for frequency-domain parameters of HRV, differences observed in baseline between young and old animals were preserved after sympathetic block (Table S2 in the Supplemental Data).

By nonlinear analysis (see Fig S7 and Table S2 in the Supplemental Data), beat-to-beat interval variability (SD1) was enhanced with propranolol only in young mice, as observed for RMSDD. In contrast, long-term RR interval variability (SD2) was enhanced in both groups of animals, preserving differences observed in baseline condition. The index of parasympathetic/sympathetic balance SD1/SD2 decreased in old mice, and a similar trend was observed in young animals ($P = 0.057$).

These results indicate that under our experimental conditions, sympathetic tone is active in young and old animals and operates by increasing heart rate and attenuating HRV. Inhibition of sympathetic tone reduced dissimilarities of RR interval duration between young and old mice, but it preserved differences of HRV observed with age. Thus, these findings tend to suggest that parasympathetic activity, which is unmasked in the presence of propranolol, is critical in mediating age-related alterations of HRV observed here.

To gain information on the consequences of parasympathetic tone in young and old animals, the muscarinic acetylcholine receptor antagonist atropine was employed (17). As reported in Table S3 in the Supplemental Data and summarized in Fig. 2*C*, parasympathetic blockade slightly decreases average RR interval duration in young mice by 2 ± 2% but had no effects in old animals, resulting in the preservation of RR interval differences for the two groups observed under baseline condition (Fig. 3*D*). Moreover, atropine decreased SDRR (by 19 ± 46%) in young but not in old mice, whereas RMSSD was reduced exclusively in old.

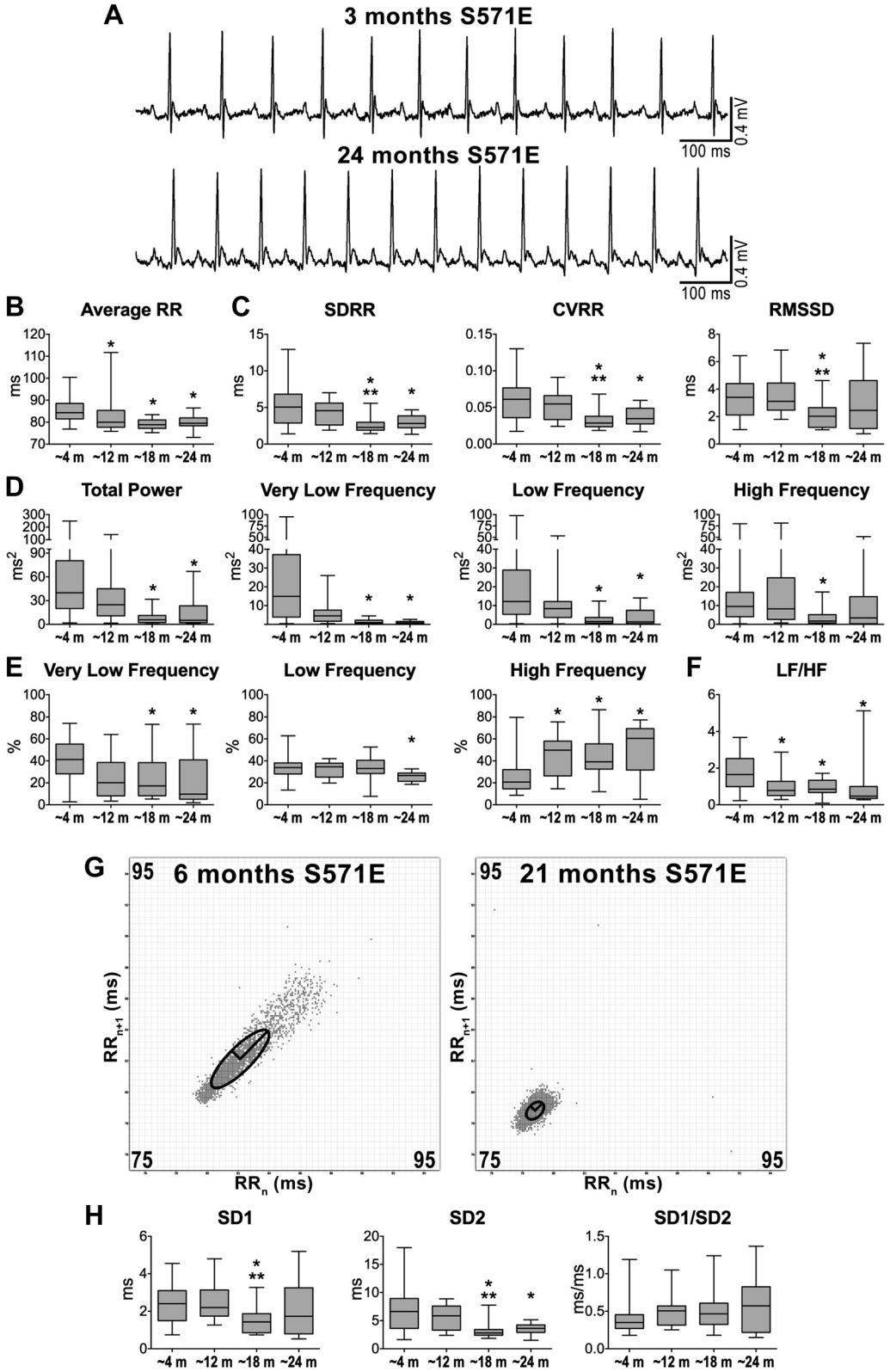

Fig. 3. Altered sodium channel function and heart rate properties with age. *A*: ECGs recorded in genetically engineered S571E male mice. Traces obtained in mice at 3 and 24 mo of age are shown. *B*: data for average RR interval duration in S571E male mice at different age intervals. SDRR, standard deviation (SD) of RR intervals; CVRR, coefficient of variation of RR intervals; RMSSD, square root of the mean of the squared differences between adjacent RR. *C*: data for time-domain parameters of heart rate variability (HRV). *D*: data for frequency-domain parameters of HRV; m, months. *E*: frequency bands normalized by total power. *F*: data for low frequency-to-high frequency (LF/HF) ratio. *G*: Poincaré plots obtained from ECGs recorded from male S571E mice at 6 and 21 mo of age. RR_n and RR_{n+1} axes span from 75 to 95 ms. *H*: data for nonlinear indexes obtained from Poincaré plots from S571E mice at different ages. Quantitative data shown in *B–D* and *F* were obtained from male S571E mice at ~4 mo ($n = 51$), ~12 mo ($n = 14$), ~18 mo ($n = 18$), and ~24 mo ($n = 14$) of age. Data are presented as medians and interquartile ranges. *$P < 0.05$ vs. ~4 m; **$P < 0.05$ vs. ~12 mo.

Parasympathetic blockade reduced very low-frequency components of RR variability in both young and old animals and low-frequency components only in young mice. The LF/HF ratio and normalized parameters of frequency bands were altered exclusively in young animals. Overall, for frequency-domain parameters of HRV, differences observed in baseline were preserved with parasympathetic block (Table S3 in the Supplemental Data).

By nonlinear analysis (see Fig S8 and Table S3 in the Supplemental Data), there were no significant changes in SD1 with atropine, whereas SD2 was significantly reduced exclusively in young animals. SD1/SD2 increased exclusively in young mice following atropine administration and the age-related difference for this parameter was abrogated.

Results obtained with atropine indicate that young and old animals are differently affected by parasympathetic blockade. Inhibition of the parasympathetic axis increases heart rate and reduces HRV only in young animals. This differential response to parasympathetic blockade leads to an attenuation of differences observed between young and old mice at baseline.

Overall, these findings suggest that, under experimental conditions used here, the sympathetic input is equally effective in young and old animals in regulating basal heart rate and HRV, whereas parasympathetic input appears to be attenuated in old mice with respect to young, possibly reflecting alterations of sympathovagal balance with age.

Effects of aging and altered sodium channel function on heart rate and HRV. To evaluate whether altered sodium channel function interferes with HR, HRV, and adaptation occurring with age, male mice with a phosphomimetic mutation of the sodium channel Nav1.5 at a CaMKII phosphorylation site (S571E mice) resulting in enhanced late sodium current (I_{NaL}) and prolongation of the action potential in atrial and ventricular myocytes (18, 19), were employed. By ECG, young S571E mice presented protracted electrical repolarization with respect to C57Bl/6 (Fig. S9 in the Supplemental Data). Mice at 3–7 (~4 mo), 11–16 (~12 mo), 18–19 (~18 mo), and 20–25 (~24 mo) mo of age were studied over a period of 10 min using electrocardiographic recordings in the conscious state. Average RR interval duration was maximal at ~4 mo and gradually decreased at ~12 to ~24 mo (Fig. 3, *A* and *B*). By time-domain variable analysis, standard deviation of RR intervals (SDRR) and coefficient of variance of RR intervals (CVRR) were maximal at ~4 and ~12 mo and decreased for animals at older age (Fig. 3*C*). In contrast, RMSSD was preserved at various time points, with the exception of animals at ~18 mo that presented reduced short-term variability. Total power, very low-, and low-frequency components of RR interval variation were maximal at ~4 mo and decreased at ~18 and ~24 mo, whereas high-frequency (HF) components were comparable in aging mice with the exception of ~18 mo animals (Fig. 3*D*). When normalized with respect to total power, very low- and low-frequency components were reduced in old animals, whereas normalized high-frequency components progressively increased and reached a maximum at ~24 mo (Fig. 3*E*). The sympathovagal balance index LF/HF ratio was maximal at ~4 mo and significantly decreased at later stages (Fig. 3*F*).

With Poincaré plots, clusters of data points for young and old S571E mice appeared differently distributed, based on dissimilarities in RR interval duration and its variability (Fig. 3*G*). Quantitatively, SD1 was comparable at the various age intervals, with the exception of animals at ~18 mo, which presented reduced SD1 (Fig. 3*H*). In contrast, SD2 was maximal at ~4 and ~12 mo and decreased thereafter. As a result, SD1/SD2 was relatively preserved with age. Therefore, aging in mice with altered sodium channel function is associated with progressive increase of heart rate and reduction of HRV.

Aging, altered sodium channel function, and modulation of heart rate by autonomic nerve activity. To establish the contribution of the autonomic nervous system on heart rate properties of mice with altered sodium channel function, ECG recordings in the conscious state were obtained in male S571E mice at 5–7 (young) and 20–29 mo (old) of age, at baseline and after administration of propranolol and atropine, to achieve combined autonomic blockade (17, 37, 52). As reported in Table S4 in the Supplemental Data, blockade of the autonomic nervous system increased average RR interval duration in young (12 ± 5%) and old (13 ± 5%) S571E mice, and the reduced RR interval with age observed at baseline was preserved after autonomic blockade. Additionally, block of the autonomic nervous system reduced SDRR (by 33 ± 39%) in young animals, but this intervention had no effects in old mice, resulting in attenuation of differences observed for the two groups of mice under baseline condition. Additionally, RMSDD was not affected by combined administration of the two drugs.

By frequency domain analysis, combined autonomic block in young S571E animals reduced total power and all components of RR variability. In contrast, this intervention had no major consequences on frequency-domain components in old animals. However, the LF/HF ratio and normalized parameters of frequency bands were altered in both groups of mice after administration of the two blockers.

By nonlinear analysis, beat-to-beat interval variability (SD1) was not affected in young and old S571E mice after autonomic blockade. In contrast, only in young animals, long-term RR interval variability (SD2) decreased, whereas SD1/SD2 increased. Changes induced by combined autonomic block abrogated differences between the two groups of mice observed under baseline condition.

Overall, these results indicate that combined sympathetic and parasympathetic blockade prolongs RR interval in young and old S571E mice but reduces HRV exclusively in young animals, attenuating age-related differences observed with intact autonomic nervous tone. The persistence of shorter RR interval duration in old S571E mice following combined sympathetic and parasympathetic blockade suggests that alterations of intrinsic mechanisms of pacemaker function are responsible for higher heart rate in aged S571E mice, whereas autonomic modulations does not directly participate to the process.

Consequences of altered sodium channel function on heart rate properties in young and old mice. To establish the consequences of altered sodium channel function on heart rate properties, a direct comparison between S571E mice and their corresponding wild-type control C57Bl/6 mice at young (~4 mo) and old (~24 mo) age was performed (see Table S5 in the Supplemental Data). With respect to C57Bl/6, average RR interval duration was 5% larger in S571E mice at ~4 mo. Similarly, time-domain, frequency-domain, and nonparametric indexes of HRV were larger in S571E mice at ~4 mo. Interestingly, the relative contribution of very low-, low-, and high-frequency bands to total power were similar in young C57Bl/6 and S571E mice. Also, LF/HF and SD1/SD2 ratios were comparable in the two groups of animals at ~4 mo.

At ~24 mo of age, average RR interval duration was 6% shorter in S571E mice, with respect to C57Bl/6. Moreover, HRV parameters and indexes indicative of sympathovagal balance were largely comparable between the two groups of

aged mice, although CVRR and SD2 were larger in S571E animals.

Thus, altered sodium channel function results in lower heart rate in young animals, whereas in old mice heart rate is increased. Additionally, altered sodium channel function and consequent reduced heart rate appear to promote enhanced HRV in young mice, a condition that is lost with age.

Inhibition of the late sodium current and heart rate properties in S571E mice. To establish whether the increase in late sodium current (I_{NaL}) associated with the phosphomimetic mutation of Nav1.5 in S571E mice was involved in the depression of heart rate and enhanced HRV in young animals, I_{NaL} was blocked in vivo with GS967, a selective I_{NaL} inhibitor (7). Moreover, based on the documentation of an inverse correlation between heart rate and HRV (23, 40), the possibility was raised that high HRV observed in S571E mice was secondary to depressed heart rate. For this purpose, ECGs were collected in S571E mice before and after administration of GS967, and data disaggregated based on animal's heart rate before administration of the drug (Fig. 4, *A* and *B*). Specifically, mice with heart rate below or above the median value for the entire group were separated in two cohorts. Interestingly, before administration of the drug (baseline), S571E mice with high heart rate presented attenuated HRV indexes with respect to S571E mice with low heart rate (Fig. 4*C* and Table S6 in the Supplemental Data).

For S571E mice with low heart rate, I_{NaL} inhibition decreased average RR interval duration (by 5 ± 5%) and substantially reduced all HRV parameters (see Fig. 4*C* and Table 6 in the Supplemental Data). Interestingly, LF/HF and SD1/SD2 ratios, reflecting the balance of sympathetic and parasympathetic axes, were not affected by I_{NaL} inhibition. In contrast, in S571E animals with high heart rate, GS967 administration increased average RR interval duration (by 3 ± 5%) but had no consequences on HRV parameters and LF/HF and SD1/SD2 ratios.

Thus, enhanced I_{NaL} is involved in the depression of heart rate and increases HRV in S571E mice. The lack of changes in indexes of sympathovagal balance in S571E mice after inhibition of I_{NaL} tends to suggest that heart rate in S571E young mice modulates HRV, a phenomenon that has been attributed to the differential impact of perturbing ionic currents on SAN function at low and high discharging rates (40).

Aging, heart rate variability, and ventricular ectopy. To establish whether the declined HRV with aging in C57Bl/6 and S571E mice was coupled with appearance of ventricular ectopy, the occurrence of premature ventricular complexes (PVCs) during the 10-min acquisition period was evaluated. The number of animals displaying isolated or recurrent PVCs (Fig. 5, *A* and *B*) increased progressively with age in a comparable manner in C57Bl/6 and S571E mice (Fig. 5*C*). Ventricular tachycardia and atrial fibrillation were not observed. Animals with PVC(s) in the C57Bl/6 cohort tended to have larger average RR interval duration with respect to the entire group of aging mice ($P = 0.06$), whereas S571E with PVC(s) had a significantly shorter average RR interval in comparison to the entire aging group (Fig. 5*D*). No alterations of heart rate variability parameters were noted for animals with PVC(s). Moreover, by bivariate correlation analysis, occurrence of PVCs was weakly but significantly associated with aging in C57Bl/6 ($r = 0.25$, $P < 0.001$) and S571E mice ($r = 0.21$, $P < 0.05$). A negative correlation of PVC(s) occurrence with average RR reached significant level in S571E mice ($r = -0.2$, $P < 0.05$), whereas a tendency for a positive correlation in C57Bl/6 was observed ($r = 0.17$, $P = 0.06$). No major significant correlations were found with respect to HRV parameters for the two strains of mice (Table S7 in the Supplemental Data).

To obtain information on the possibility that S571E mice with altered sodium channel function develop lethal arrhythmic events not captured during the 10-min monitoring, we assessed survival of aging animals. For both male and female mice, no

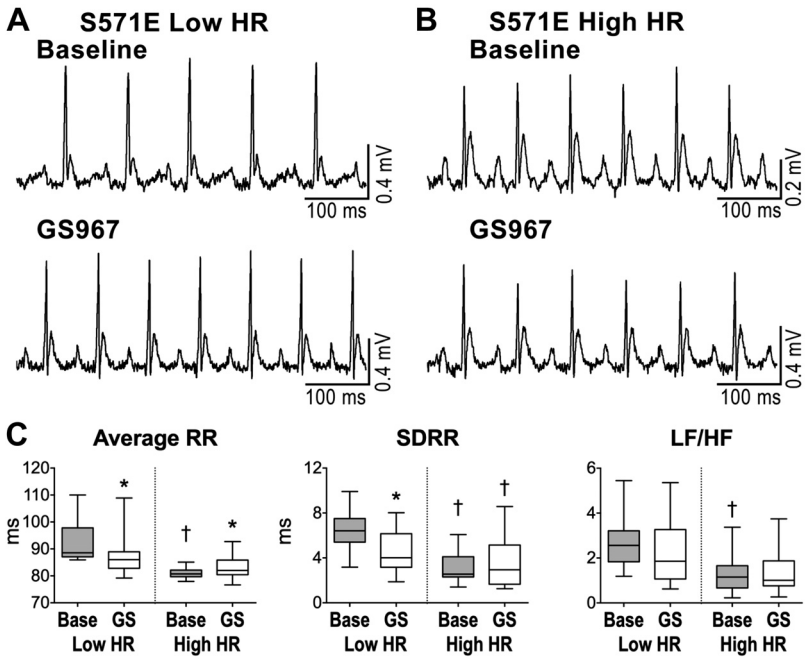

Fig. 4. Effects of inhibition of late sodium current (I_{NaL}) in mice with altered sodium channel function. *A* and *B*: ECGs recorded in S571E male mice at 4 mo with low heart rate (low HR; *A*) and high heart rate (high HR; *B*) before (baseline) and following inhibition of I_{NaL} with GS967. *C*: data for average RR interval duration, standard deviation of RR intervals (SDRR), and low frequency-to-high frequency (LF/HF) ratio in in young S571E mice with low HR ($n = 16$) and young S571E mice with high HR ($n = 16$) before (base) and after inhibition of I_{NaL} with GS967 (GS). Data are presented as medians and interquartile ranges. *$P < 0.05$ vs. baseline; †$P < 0.05$ vs. low HR under the same experimental condition.

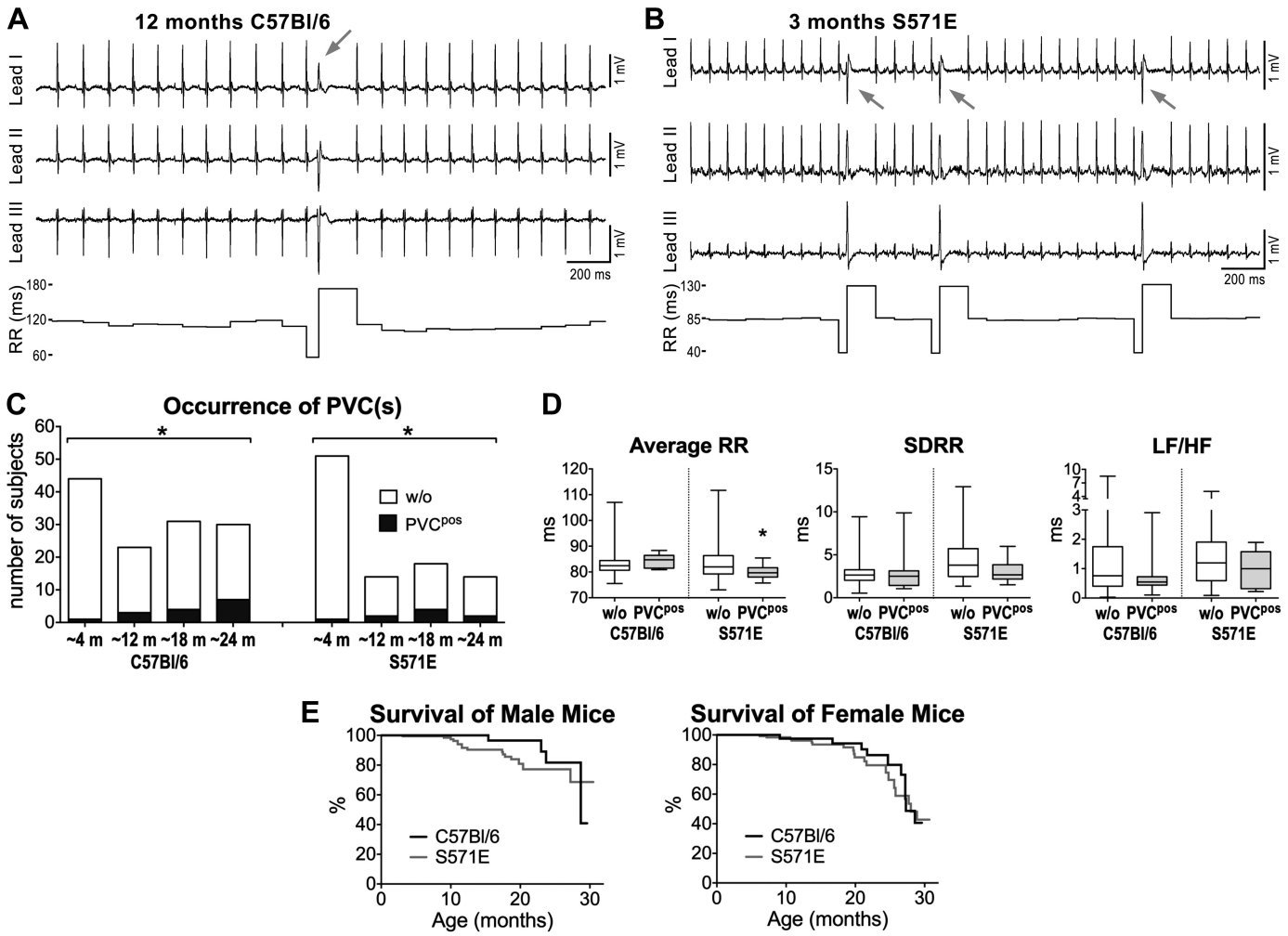

Fig. 5. Ventricular ectopy, aging, heart rate variability (HRV), and survival. *A*: ECGs traces and RR interval duration for a C57Bl/6 mouse at 12 mo of age document the appearance of an isolated premature ventricular complex (PVC; gray arrow). *B*: ECGs traces and RR interval duration for a S571E mouse at 3 mo of age document the appearance of recurrent PVCs (gray arrows). *C*: quantitative data for aging C57Bl/6 and S571E mice without (w/o) or presenting isolated or multiple PVCs (PVC^{pos}). m, months. $^*P < 0.05$ vs. ~4 mo using χ^2-test for trend. *D*: quantitative data for HRV parameters in C57Bl/6 and S571E mice without ($n = 113, 88$) and with PVC(s) (PVC^{pos}, $n = 15, 9$). SDRR, standard deviation of RR intervals; LF/HF, low frequency-to-high frequency ratio. $^*P < 0.05$ vs. w/o. *E*: survival curves for male C57Bl/6 ($n = 79$) and S571E ($n = 185$) mice and for female C57Bl/6 ($n = 40$) and S571E ($n = 158$) mice. For the 2 sexes, survival curves for the 2 genotypes were not significantly different using Gehan–Breslow–Wilcoxon and log-rank (Mantel–Cox) tests.

significant differences were observed between C57Bl/6 and S571E strains (Fig. 5*E*).

Overall, occurrence of ventricular ectopy increases with age in mice with intact or altered sodium channel function. The direct and inverse association between occurrence of PVC(s) and RR interval duration in C57Bl/6 and S571E mice, respectively, appears to reflect the heart rate properties of aged mice for these two genotypes.

DISCUSSION

Results of the current study obtained with restraint methodology reveal that aging in rodents is associated with attenuation of HRV, a condition that appears to be secondary to altered balance of sympathetic and vagal inputs. Reduction of HRV occurs relatively early in the mouse life, being parameters of long-term RR interval variability decreased at ~12 mo of age. Interestingly, indexes of short-term variability, including the time-domain RMSSD and the nonlinear parameter SD1, are preserved with age, pointing to the possibility that the rapidly acting component of parasympathetic tone, which accounts for instantaneous beat-to-beat variations (1, 43), is relatively maintained with aging. This possibility is corroborated by the conserved levels of high-frequency components of RR interval variability, which is mainly under the influence of parasympathetic tone (43, 48). The notion that sympathovagal input is affected by age is substantiated by alterations of LF/HF and SD1/SD2 ratios. Specifically, for animals at ~18 and ~24 mo of age, LF/HF decreases, whereas SD1/SD2 increases. These ratios indicate that the relative contribution of the two arms of the autonomic nervous system to the modulation of heart rhythm under our experimental conditions reaches a new equilibrium in aged mice. However, due to the participation of parasympathetic input to modulation of both low- and high-frequency components, interpretation of changes of LF/HF ratio are rather challenging (10). Combined autonomic block with propranolol and atropine, largely reduced HRV in young mice, whereas no major effects were observed in old animals, strengthening the possibility that the response to sympathetic

and parasympathetic arms is attenuated with age. In this regard, reduced responsiveness of the isolated SAN from aged mice to neurotransmitters has been reported (30, 60), and this condition may represent the basis for the in vivo behavior of old animals observed here. Importantly, combined autonomic blockade largely abrogated differences of HRV between young and old animals, confirming the central role of autonomic nervous inputs in determining age-related alterations of RR interval properties observed here.

Targeted block of the sympathetic axis with propranolol enhanced HRV in young mice, whereas effects in old animals were less prominent. This intervention preserved differences between young and old animals observed with intact autonomic nervous system. These results highlight the role of sympathetic input in containing HRV and also suggest that parasympathetic tone alone is sufficient to reveal age-related alterations of HRV. Interestingly, inhibition of the parasympathetic axis with atropine substantially reduced HRV in young mice and, to a smaller extent, in old animals. As a consequence, differences between the two age groups observed in baseline were attenuated with parasympathetic block. Thus, interventions aimed at masking the parasympathetic arm of the autonomic nervous system tend to eliminate age-related alterations of HRV, substantiating the possibility that decreased parasympathetic input is a critical determinant of the altered sympathovagal balance occurring with age.

Experimental studies have documented that aging is associated with alterations of action potential duration, diastolic depolarization rate, and maximum diastolic potential of the SAN (2, 26, 45, 57). These adjustments are coupled with modifications of voltage and calcium clock mechanisms and their response to neurotransmitters (26, 30, 50, 60), together with structural and anatomical changes of the nodal tissue (39, 51, 58). Thus, a number of factors involved in pacemaker function are affected with age, and our results clearly document that intrinsic heart rate is reduced in old C57Bl/6 mice, a result that is in line with previous findings (30, 60). Interestingly, propranolol decreased heart rate in both young and old animals, whereas atropine increased heart rate only in young. These results indicate that heart rate in rodents, and particularly in the presence of physical and emotional stress associated with the restrain method used here (20, 31, 32, 35), is largely influenced by sympathetic tone, whereas the parasympathetic axis has minor influence on beating frequency in young mice and has no detectable effects on heart rate in old animals. These findings raise the possibility that factors underlying the reduction of heart rate with age render ineffective the modulatory action of acetylcholine on SAN discharge, although reduced input of and/or responsiveness to the parasympathetic tone appear to be mechanisms involved here.

Results obtained from S571E mice with enhanced late sodium current (I_{NaL}) and prolongation of the action potential in atrial and ventricular myocytes (18, 19) offer important evidence on the contribution of sodium channels to SAN function. Moreover, analysis and interventions directed to establish age-related alterations of HRV in S571E mice substantiate findings obtained in wild-type animals. As observed in C57Bl/6, HRV decreased with age in S571E mice, together with alteration of the balance between sympathetic and parasympathetic arms.

Mechanisms underlying the slower firing rate of the SAN of S571E young mice have not been addressed here and require further investigation. The enhanced sodium influx via I_{NaL} may increase cytosolic sodium load in SAN cells stimulating Na^+/K^+-ATPase and favoring reverse mode activity of the Na^+/Ca^{2+} exchange, factors promoting hyperpolarization of maximum diastolic potential and slowing of firing rate. Moreover, enhanced sodium load interferes with calcium extrusion via the Na^+/Ca^{2+} exchange, resulting in increased intracellular calcium levels. In this regard, effects of enhanced sodium and consequent calcium load on SAN cell automaticity have been tested by others (53) by using the digitalis glycoside digoxigenin, which inhibits sodium extrusion via the Na^+/K^+-ATPase and increases intracellular sodium. It was found that the initial increase in intracellular sodium level was associated with faster SAN cell discharge, whereas further sodium increase resulted in slower firing rate and enhanced cycle length variability (53). These events were attributed to the consequences of reduced sodium and calcium electrochemical gradient on mechanisms coupling calcium clock and transmembrane ionic fluxes. Thus, enhanced sodium load in SAN cell may represent the initial event conditioning heart rhythm behavior of young S571E mice.

The findings that aging in S571E mice is associated with increased heart rate renders the scenario of putative player involved in the process even more intricated. Despite the lack of knowledge on these aspects, the increased heart rate in aged S571E mice, which is opposed to the decrease observed in C57Bl/6, represents a peculiar adaptation of the old heart with repercussions on maximal heart rate and maximal aerobic capacity, critically affected in the elderly.

The notion that altered Nav1.5 behavior in S571E mice affects heart rate has implications for the patient populations with gain-of-function mutations of *SCN5A*, the gene encoding for sodium channel Nav1.5 and manifesting with long QT syndrome type 3 (LQT3). It has been reported that in children with LQT3, heart rate at rest tends to be lower in carriers than in noncarriers (6). Similarly, in adult patients with long QT syndrome, average RR interval was prolonged in comparison to controls and maximal in LQT3 carriers, with respect to LQT1 and LQT2 (44). However, some of the adult LQT patients included in the study were treated with β-blockers, imposing caution on the interpretation of these results. Nonetheless, other two clinical studies confirmed that heart rate is lower in LQT patients not treated with β-blockers, with respect to controls (42, 49). Discordant results with respect to HRV parameters in LQT patients were reported by the two latter investigations. However, reduction of LF/HF ratio was found in both studies, which was interpreted, in light of the slower heart rate, as secondary to reduced sympathetic input in patients with LQT (42, 49). Although we have no indication that altered sodium channel function in young mice is coupled with attenuated sympathetic tone, our finding supports the notion the decreased heart rate associated with gain-of-function mutations of the sodium channel is an intrinsic property of the SAN and is independent from the autonomic control, a condition that may apply to LQT3 patients.

We previously reported that aged mice have prolonged QT interval duration which is accounted, at least in part, by lengthened repolarization of the action potential and enhanced I_{NaL} in myocytes (52). Importantly, these cellular alterations influence performance of the aged myocardium of rodents and large mammals (52, 55). No significant reductions of Nav1.5

transcripts and proteins were identified with aging (52), pointing to the possibility that post-translational modifications of sodium channel underlie the increase of I_{NaL}. The phosphomimetic mutation of Nav1.5 in S571E mice manifests with prolonged QT interval in animals at young age and, at the cellular level, with enhanced I_{NaL} and protracted action potential duration, features that have been observed in aged C57Bl/6 mice (52). Moreover, young S571E animals mimic the slower heart rate of aged control mice, raising the possibility that altered I_{NaL} may contribute, together with already identified factors, to the depressed function of the aged pacemaker tissue. Further investigations are needed to clarify this possibility.

Aging in C57Bl/6 mice was coupled with increased incidence of ventricular ectopy and a comparable behavior was found in S571E mice. Additionally, survival curves for the two genotypes were not different, diminishing the possibility that sudden cardiac death occurs at a higher rate in animals with phosphomimetic mutation of Nav1.5. These findings, however, do not rule out the notion that enhanced I_{NaL} constitutes a substrate for arrhythmia. In fact, a previous study documented that catecholaminergic stress by epinephrine administration in combination with treadmill exercise enhanced occurrence of PVCs and ventricular tachycardia in S571E young mice, with respect to control animals (18). Bivariate analysis documented that occurrence of ventricular ectopy had no strong correlations with HRV parameters. A tendency for a positive and negative correlation with average RR duration for C57Bl/6 and S571E mice, respectively, and a negative correlation with low-frequency component of RR variation for both group of animals were observed. However, it appears that these trends are secondary to the characteristics of these HRV parameters in aged mice.

Our findings in mice are in line with clinical studies (5, 22, 56, 59, 62) addressing the consequences of aging on HRV. A comparison of healthy subjects at age ranging from 10 to 19 to 80–99 yr revealed that standard deviation of normal RR interval decreased significantly at 30–39 yr of age and reached a minimum at 80–99 yr (59). A similar behavior was observed with respect to short-term HRV, measured by RMSSD. Interestingly, in longitudinal studies over a period of ~15-yr (22, 56) low-frequency components of RR interval duration and LF/HF ratio were decreased by age. As detected clinically, we have found that SDRR in mice is already decreased at ~12 mo of age, reiterating, at least in part, the early decline of HRV observed in humans. Moreover, the decrease of low frequency and LF/HF ratio observed in aging mice is consistent with results of longitudinal clinical studies. In contrast, we did not detect alterations of RMSSD in old animals, which may reflect a different role of the parasympathetic axis in the aging process of human and rodents.

Study limitations. Electrophysiological tests in mice have largely employed acquisition of ECG signals by telemetry (18, 37, 38, 52, 54), an approach that allows for long-term monitoring of conscious animals in their natural living environment (21), but that requires surgical implantation of telemetric biopotential transmitters. In contrast, the ECG-tunnel device allows for screening of a large number of mice for brief monitoring periods, without the need of animal surgery and instrumentation. To our knowledge, this is the first study evaluating HRV in the conscious state in mice using an ECG-tunnel device. Our data complement results of previous investigations assessing heart rhythm dynamics in conscious mice using telemetry (17, 38) or animals under light general anesthesia (60) and, ex vivo, using isolated, intact SAN preparations (30). A limitation of the ECG-tunnel system is represented by the restraint method imposed on animals during the acquisition process. This approach has an impact on sympathovagal balance, as confirmed by the shorter-average RR interval duration observed here with respect to conscious telemetric assessments (17, 38, 52). In this regard, it has been reported that restraint causes physical and emotional stress and activates the sympathoadrenal medullary system (24) promoting stress-induced tachycardia (20, 31, 32, 35). Importantly, the response to restraint may be affected by animal age (61), a factor perhaps contributing to the age-related alterations detected in our study.

In conclusion, our findings indicate that aging in mice is coupled with reduced heart rate and attenuation of HRV, possibly as consequence of deterioration of SAN function and altered balance of sympathetic and vagal inputs under our experimental conditions, respectively. Interestingly, in mice with altered sodium channel function, heart rate is slower at young age and progressively become faster at old age, pointing to sodium channel as key modulator of SAN discharge.

GRANTS

This work was supported by National Institute of Health Grant R01AG055407, American Heart Association Grant 19TPA34850067, and intramural resources at New York Medical College (NYMC), including funds from the NYMC Translational Science Institute. M. Comelli was supported by Overworld Scholarship of the University of Parma.

DISCLOSURES

No conflicts of interest, financial or otherwise, are declared by the authors.

AUTHOR CONTRIBUTIONS

M.C., M.M., O.M., and M.R. conceived and designed research; M.C., D.O.C., E.P., A.P., and M.R. performed experiments; M.C., M.M., E.P., A.P., O.M., and M.R. analyzed data; M.C., M.M., J.T.J., and M.R. interpreted results of experiments; M.C., M.M., O.M., and M.R. prepared figures; M.C. and M.R. drafted manuscript; M.C., M.M., D.O.C., J.T.J., O.M., and M.R. edited and revised manuscript; M.C., M.M., D.O.C., E.P., A.P., P.J.M., T.J.H., J.T.J., O.M., and M.R. approved final version of manuscript.

REFERENCES

1. **Alings AM, Bouman LN.** Electrophysiology of the ageing rabbit and cat sinoatrial node–a comparative study. *Eur Heart J* 14: 1278–1288, 1993. doi:10.1093/eurheartj/14.9.1278.
2. **Alves Bento AS, Bacic D, Saran Carneiro J, Nearing BD, Fuller H, Justo FA, Rajamani S, Belardinelli L, Verrier RL.** Selective late INa inhibition by GS-458967 exerts parallel suppression of catecholamine-induced hemodynamically significant ventricular tachycardia and T-wave alternans in an intact porcine model. *Heart Rhythm* 12: 2508–2514, 2015. doi:10.1016/j.hrthm.2015.07.025.
3. **Anderson LL, Thompson CH, Hawkins NA, Nath RD, Petersohn AA, Rajamani S, Bush WS, Frankel WN, Vanoye CG, Kearney JA, George AL Jr.** Antiepileptic activity of preferential inhibitors of persistent sodium current. *Epilepsia* 55: 1274–1283, 2014. doi:10.1111/epi.12657.
5. **Antelmi I, de Paula RS, Shinzato AR, Peres CA, Mansur AJ, Grupi CJ.** Influence of age, gender, body mass index, and functional capacity on heart rate variability in a cohort of subjects without heart disease. *Am J Cardiol* 93: 381–385, 2004. doi:10.1016/j.amjcard.2003.09.065.
6. **Beaufort-Krol GC, van den Berg MP, Wilde AA, van Tintelen JP, Viersma JW, Bezzina CR, Bink-Boelkens MT.** Developmental aspects of long QT syndrome type 3 and Brugada syndrome on the basis of a single SCN5A mutation in childhood. *J Am Coll Cardiol* 46: 331–337, 2005. doi:10.1016/j.jacc.2005.03.066.

7. **Belardinelli L, Liu G, Smith-Maxwell C, Wang WQ, El-Bizri N, Hirakawa R, Karpinski S, Li CH, Hu L, Li XJ, Crumb W, Wu L, Koltun D, Zablocki J, Yao L, Dhalla AK, Rajamani S, Shryock JC.** A novel, potent, and selective inhibitor of cardiac late sodium current suppresses experimental arrhythmias. *J Pharmacol Exp Ther* 344: 23–32, 2013. doi:10.1124/jpet.112.198887.
8. **Benjamin EJ, Muntner P, Alonso A, Bittencourt MS, Callaway CW, Carson AP, Chamberlain AM, Chang AR, Cheng S, Das SR, Delling FN, Djousse L, Elkind MSV, Ferguson JF, Fornage M, Jordan LC, Khan SS, Kissela BM, Knutson KL, Kwan TW, Lackland DT, Lewis TT, Lichtman JH, Longenecker CT, Loop MS, Lutsey PL, Martin SS, Matsushita K, Moran AE, Mussolino ME, O'Flaherty M, Pandey A, Perak AM, Rosamond WD, Roth GA, Sampson UK, Satou GM, Schroeder EB, Shah SH, Spartano NL, Stokes A, Tirschwell DL, Tsao CW, Turakhia MP, VanWagner LB, Wilkins JT, Wong SS, Virani SS; American Heart Association Council on Epidemiology and Prevention Statistics Committee and Stroke Statistics Subcommittee.** Heart Disease and Stroke Statistics-2019 Update: A Report From the American Heart Association. *Circulation* 139: e56–e528, 2019. doi:10.1161/CIR.0000000000000659.
9. **Berul CI, McConnell BK, Wakimoto H, Moskowitz IP, Maguire CT, Semsarian C, Vargas MM, Gehrmann J, Seidman CE, Seidman JG.** Ventricular arrhythmia vulnerability in cardiomyopathic mice with homozygous mutant Myosin-binding protein C gene. *Circulation* 104: 2734–2739, 2001. doi:10.1161/hc4701.099582.
10. **Billman GE.** The LF/HF ratio does not accurately measure cardiac sympatho-vagal balance. *Front Physiol* 4: 26, 2013. doi:10.3389/fphys.2013.00026.
11. **Blain G, Meste O, Blain A, Bermon S.** Time-frequency analysis of heart rate variability reveals cardiolocomotor coupling during dynamic cycling exercise in humans. *Am J Physiol Heart Circ Physiol* 296: H1651–H1659, 2009. doi:10.1152/ajpheart.00881.2008.
12. **Borghetti G, Eisenberg CA, Signore S, Sorrentino A, Kaur K, Andrade-Vicenty A, Edwards JG, Nerkar M, Qanud K, Sun D, Goichberg P, Leri A, Anversa P, Eisenberg LM, Jacobson JT, Hintze TH, Rota M.** Notch signaling modulates the electrical behavior of cardiomyocytes. *Am J Physiol Heart Circ Physiol* 314: H68–H81, 2018. doi:10.1152/ajpheart.00587.2016.
13. **Christou DD, Seals DR.** Decreased maximal heart rate with aging is related to reduced beta-adrenergic responsiveness but is largely explained by a reduction in intrinsic heart rate. *J Appl Physiol (1985)* 105: 24–29, 2008. doi:10.1152/japplphysiol.90401.2008.
14. **D'Souza A, Bucchi A, Johnsen AB, Logantha SJ, Monfredi O, Yanni J, Prehar S, Hart G, Cartwright E, Wisloff U, Dobryznski H, DiFrancesco D, Morris GM, Boyett MR.** Exercise training reduces resting heart rate via downregulation of the funny channel HCN4. *Nat Commun* 5: 3775, 2014. doi:10.1038/ncomms4775.
15. **Fenske S, Pröbstle R, Auer F, Hassan S, Marks V, Pauza DH, Biel M, Wahl-Schott C.** Comprehensive multilevel in vivo and in vitro analysis of heart rate fluctuations in mice by ECG telemetry and electrophysiology. *Nat Protoc* 11: 61–86, 2016. doi:10.1038/nprot.2015.139.
16. **Fishman M, Jacono FJ, Park S, Jamasebi R, Thungtong A, Loparo KA, Dick TE.** A method for analyzing temporal patterns of variability of a time series from Poincare plots. *J Appl Physiol (1985)* 113: 297–306, 2012. doi:10.1152/japplphysiol.01377.2010.
17. **Gehrmann J, Hammer PE, Maguire CT, Wakimoto H, Triedman JK, Berul CI.** Phenotypic screening for heart rate variability in the mouse. *Am J Physiol Heart Circ Physiol* 279: H733–H740, 2000. doi:10.1152/ajpheart.2000.279.2.H733.
18. **Glynn P, Musa H, Wu X, Unudurthi SD, Little S, Qian L, Wright PJ, Radwanski PB, Gyorke S, Mohler PJ, Hund TJ.** Voltage-Gated Sodium Channel Phosphorylation at Ser571 Regulates Late Current, Arrhythmia, and Cardiac Function In Vivo. *Circulation* 132: 567–577, 2015. doi:10.1161/CIRCULATIONAHA.114.015218.
19. **Greer-Short A, Musa H, Alsina KM, Ni L, Word TA, Reynolds JO, Gratz D, Lane C, El-Refaey M, Unudurthi S, Skaf M, Li N, Fedorov VV, Wehrens XH, Mohler PJ, Hund TJ.** Calmodulin kinase II regulates atrial myocyte late sodium current, calcium handling, and atrial arrhythmia. *Heart Rhythm* 17: 503–511, 2020. doi:10.1016/j.hrthm.2019.10.016.
20. **Gross V, Luft FC.** Exercising restraint in measuring blood pressure in conscious mice. *Hypertension* 41: 879–881, 2003. doi:10.1161/01.HYP.0000060866.69947.D1.
21. **Ho D, Zhao X, Gao S, Hong C, Vatner DE, Vatner SF.** Heart rate and electrocardiography monitoring in mice. *Curr Protoc Mouse Biol* 1: 123–139, 2011. doi:10.1002/9780470942390.mo100159.
22. **Jokinen V, Sourander LB, Karanko H, Mäkikallio TH, Huikuri HV.** Changes in cardiovascular autonomic regulation among elderly subjects: follow-up of sixteen years. *Ann Med* 37: 206–212, 2005. doi:10.1080/07853890510007331.
23. **Kazmi SZ, Zhang H, Aziz W, Monfredi O, Abbas SA, Shah SA, Kazmi SS, Butt WH.** Inverse correlation between heart rate variability and heart rate demonstrated by linear and nonlinear analysis. *PLoS One* 11: e0157557, 2016. doi:10.1371/journal.pone.0157557.
24. **Kvetnanský R, Pacák K, Fukuhara K, Viskupic E, Hiremagalur B, Nankova B, Goldstein DS, Sabban EL, Kopin IJ.** Sympathoadrenal system in stress. Interaction with the hypothalamic-pituitary-adrenocortical system. *Ann N Y Acad Sci* 771: 131–158, 1995.
25. **Lakatta EG, Maltsev VA, Vinogradova TM.** A coupled SYSTEM of intracellular Ca2+ clocks and surface membrane voltage clocks controls the timekeeping mechanism of the heart's pacemaker. *Circ Res* 106: 659–673, 2010. doi:10.1161/CIRCRESAHA.109.206078.
26. **Larson ED, St Clair JR, Sumner WA, Bannister RA, Proenza C.** Depressed pacemaker activity of sinoatrial node myocytes contributes to the age-dependent decline in maximum heart rate. *Proc Natl Acad Sci USA* 110: 18011–18016, 2013. doi:10.1073/pnas.1308477110.
27. **Lei M, Jones SA, Liu J, Lancaster MK, Fung SS, Dobrzynski H, Camelliti P, Maier SK, Noble D, Boyett MR.** Requirement of neuronal- and cardiac-type sodium channels for murine sinoatrial node pacemaking. *J Physiol* 559: 835–848, 2004. doi:10.1113/jphysiol.2004.068643.
28. **Leoni AL, Marionneau C, Demolombe S, Le Bouter S, Mangoni ME, Escande D, Charpentier F.** Chronic heart rate reduction remodels ion channel transcripts in the mouse sinoatrial node but not in the ventricle. *Physiol Genomics* 24: 4–12, 2005. doi:10.1152/physiolgenomics.00161.2005.
29. **Li N, Kalyanasundaram A, Hansen BJ, Artiga EJ, Sharma R, Abudulwahed SH, Helfrich KM, Rozenberg G, Wu PJ, Zakharkin S, Gyorke S, Janssen PM, Whitson BA, Mokadam NA, Biesiadecki BJ, Accornero F, Hummel JD, Mohler PJ, Dobrzynski H, Zhao J, Fedorov VV.** Impaired neuronal sodium channels cause intranodal conduction failure and reentrant arrhythmias in human sinoatrial node. *Nat Commun* 11: 512, 2020. doi:10.1038/s41467-019-14039-8.
30. **Liu J, Sirenko S, Juhaszova M, Sollott SJ, Shukla S, Yaniv Y, Lakatta EG.** Age-associated abnormalities of intrinsic automaticity of sinoatrial nodal cells are linked to deficient cAMP-PKA-Ca(2+) signaling. *Am J Physiol Heart Circ Physiol* 306: H1385–H1397, 2014. doi:10.1152/ajpheart.00088.2014.
31. **Liu J, Wei W, Kuang H, Zhao F, Tsien JZ.** Changes in heart rate variability are associated with expression of short-term and long-term contextual and cued fear memories. *PLoS One* 8: e63590, 2013. doi:10.1371/journal.pone.0063590.
32. **Lorenz JN.** A practical guide to evaluating cardiovascular, renal, and pulmonary function in mice. *Am J Physiol Regul Integr Comp Physiol* 282: R1565–R1582, 2002. doi:10.1152/ajpregu.00759.2001.
33. **Lyashkov AE, Vinogradova TM, Zahanich I, Li Y, Younes A, Nuss HB, Spurgeon HA, Maltsev VA, Lakatta EG.** Cholinergic receptor signaling modulates spontaneous firing of sinoatrial nodal cells via integrated effects on PKA-dependent Ca(2+) cycling and I(KACh). *Am J Physiol Heart Circ Physiol* 297: H949–H959, 2009. doi:10.1152/ajpheart.01340.2008.
34. **MacDonald EA, Rose RA, Quinn TA.** Neurohumoral control of sinoatrial node activity and heart rate: insight from experimental models and findings from humans. *Front Physiol* 11: 170, 2020. doi:10.3389/fphys.2020.00170.
35. **Meijer MK, Spruijt BM, van Zutphen LF, Baumans V.** Effect of restraint and injection methods on heart rate and body temperature in mice. *Lab Anim* 40: 382–391, 2006. doi:10.1258/002367706778476370.
36. **Meo M, Meste O, Signore S, Rota M.** Novel methods for high-resolution assessment of cardiac action potential repolarization. *Biomed Signal Process Control* 51: 30–41, 2019. doi:10.1016/j.bspc.2019.02.003.
37. **Meo M, Meste O, Signore S, Sorrentino A, Cannata A, Zhou Y, Matsuda A, Luciani M, Kannappan R, Goichberg P, Leri A, Anversa P, Rota M.** Reduction in Kv current enhances the temporal dispersion of the action potential in diabetic myocytes: insights from a novel repolarization algorithm. *J Am Heart Assoc* 5: e003078, 2016. doi:10.1161/JAHA.115.003078.

38. **Moen JM, Matt MG, Ramirez C, Tarasov KV, Chakir K, Tarasova YS, Lukyanenko Y, Tsutsui K, Monfredi O, Morrell CH, Tagirova S, Yaniv Y, Huynh T, Pacak K, Ahmet I, Lakatta EG.** Overexpression of a neuronal type adenylyl cyclase (Type 8) in sinoatrial node markedly impacts heart rate and rhythm. *Front Neurosci* 13: 615, 2019. doi:10.3389/fnins.2019.00615.
39. **Moghtadaei M, Jansen HJ, Mackasey M, Rafferty SA, Bogachev O, Sapp JL, Howlett SE, Rose RA.** The impacts of age and frailty on heart rate and sinoatrial node function. *J Physiol* 594: 7105–7126, 2016. doi:10.1113/JP272979.
40. **Monfredi O, Lyashkov AE, Johnsen AB, Inada S, Schneider H, Wang R, Nirmalan M, Wisloff U, Maltsev VA, Lakatta EG, Zhang H, Boyett MR.** Biophysical characterization of the underappreciated and important relationship between heart rate variability and heart rate. *Hypertension* 64: 1334–1343, 2014. doi:10.1161/HYPERTENSIONAHA.114.03782.
41. **Mongue-Din H, Salmon A, Fiszman MY, Fromes Y.** Non-invasive restrained ECG recording in conscious small rodents: a new tool for cardiac electrical activity investigation. *Pflugers Arch* 454: 165–171, 2007. doi:10.1007/s00424-006-0197-8.
42. **Morita H, Yamanari H, Ohe T.** Evaluation of autonomic nervous activity in patients with congenital long QT syndrome by an analysis of RR variability. *Jpn Circ J* 60: 742–748, 1996. doi:10.1253/jcj.60.742.
43. **Nicolini P, Ciulla MM, De Asmundis C, Magrini F, Brugada P.** The prognostic value of heart rate variability in the elderly, changing the perspective: from sympathovagal balance to chaos theory. *Pacing Clin Electrophysiol* 35: 622–638, 2012. doi:10.1111/j.1540-8159.2012.03335.x.
44. **Perkiömäki JS, Zareba W, Couderc JP, Moss AJ.** Heart rate variability in patients with congenital long QT syndrome. *Ann Noninvasive Electrocardiol* 6: 298–304, 2001. doi:10.1111/j.1542-474X.2001.tb00122.x.
45. **Peters CH, Sharpe EJ, Proenza C.** Cardiac pacemaker activity and aging. *Annu Rev Physiol* 82: 21–43, 2020. doi:10.1146/annurev-physiol-021119-034453.
46. **Roy B, Ghatak S.** Nonlinear methods to assess changes in heart rate variability in type 2 diabetic patients. *Arq Bras Cardiol* 101: 317–327, 2013. doi:10.5935/abc.20130181.
47. **Saba S, London B, Ganz L.** Autonomic blockade unmasks maturational differences in rate-dependent atrioventricular nodal conduction and facilitation in the mouse. *J Cardiovasc Electrophysiol* 14: 191–195, 2003. doi:10.1046/j.1540-8167.2003.02454.x.
48. **Shaffer F, Ginsberg JP.** An overview of heart rate variability metrics and norms. *Front Public Health* 5: 258, 2017. doi:10.3389/fpubh.2017.00258.
49. **Shamsuzzaman AS, Ackerman MJ, Kara T, Lanfranchi P, Somers VK.** Sympathetic nerve activity in the congenital long-QT syndrome. *Circulation* 107: 1844–1847, 2003. doi:10.1161/01.CIR.0000066284.34258.59.
50. **Sharpe EJ, Larson ED, Proenza C.** Cyclic AMP reverses the effects of aging on pacemaker activity and If in sinoatrial node myocytes. *J Gen Physiol* 149: 237–247, 2017. doi:10.1085/jgp.201611674.
51. **Shiraishi I, Takamatsu T, Minamikawa T, Onouchi Z, Fujita S.** Quantitative histological analysis of the human sinoatrial node during growth and aging. *Circulation* 85: 2176–2184, 1992. doi:10.1161/01.CIR.85.6.2176.
52. **Signore S, Sorrentino A, Borghetti G, Cannata A, Meo M, Zhou Y, Kannappan R, Pasqualini F, O'Malley H, Sundman M, Tsigkas N, Zhang E, Arranto C, Mangiaracina C, Isobe K, Sena BF, Kim J, Goichberg P, Nahrendorf M, Isom LL, Leri A, Anversa P, Rota M.** Late Na(+) current and protracted electrical recovery are critical determinants of the aging myopathy. *Nat Commun* 6: 8803, 2015. doi:10.1038/ncomms9803.
53. **Sirenko SG, Maltsev VA, Yaniv Y, Bychkov R, Yaeger D, Vinogradova T, Spurgeon HA, Lakatta EG.** Electrochemical Na+ and Ca2+ gradients drive coupled-clock regulation of automaticity of isolated rabbit sinoatrial nodal pacemaker cells. *Am J Physiol Heart Circ Physiol* 311: H251–H267, 2016. doi:10.1152/ajpheart.00667.2015.
54. **Sorrentino A, Borghetti G, Zhou Y, Cannata A, Meo M, Signore S, Anversa P, Leri A, Goichberg P, Qanud K, Jacobson JT, Hintze TH, Rota M.** Hyperglycemia induces defective Ca2+ homeostasis in cardiomyocytes. *Am J Physiol Heart Circ Physiol* 312: H150–H161, 2017. doi:10.1152/ajpheart.00737.2016.
55. **Sorrentino A, Signore S, Qanud K, Borghetti G, Meo M, Cannata A, Zhou Y, Wybieralska E, Luciani M, Kannappan R, Zhang E, Matsuda A, Webster A, Cimini M, Kertowidjojo E, D'Alessandro DA, Wunimenghe O, Michler RE, Royer C, Goichberg P, Leri A, Barrett EG, Anversa P, Hintze TH, Rota M.** Myocyte repolarization modulates myocardial function in aging dogs. *Am J Physiol Heart Circ Physiol* 310: H873–H890, 2016. doi:10.1152/ajpheart.00682.2015.
56. **Tasaki H, Serita T, Irita A, Hano O, Iliev I, Ueyama C, Kitano K, Seto S, Hayano M, Yano K.** A 15-year longitudinal follow-up study of heart rate and heart rate variability in healthy elderly persons. *J Gerontol A Biol Sci Med Sci* 55: M744–M749, 2000. doi:10.1093/gerona/55.12.M744.

56a. **Task Force of the European Society of Cardiology and the North American Society of Pacing and Electrophysiology.** Heart rate variability: standards of measurement, physiological interpretation and clinical use. *Circulation* 93: 1043–1065, 1996. doi:10.1161/01.CIR.93.5.1043.

57. **Tellez JO, Mączewski M, Yanni J, Sutyagin P, Mackiewicz U, Atkinson A, Inada S, Beresewicz A, Billeter R, Dobrzynski H, Boyett MR.** Ageing-dependent remodelling of ion channel and Ca2+ clock genes underlying sino-atrial node pacemaking. *Exp Physiol* 96: 1163–1178, 2011. doi:10.1113/expphysiol.2011.057752.
58. **Thery C, Gosselin B, Lekieffre J, Warembourg H.** Pathology of sinoatrial node. Correlations with electrocardiographic findings in 111 patients. *Am Heart J* 93: 735–740, 1977. doi:10.1016/S0002-8703(77)80070-7.
59. **Umetani K, Singer DH, McCraty R, Atkinson M.** Twenty-four hour time domain heart rate variability and heart rate: relations to age and gender over nine decades. *J Am Coll Cardiol* 31: 593–601, 1998. doi:10.1016/S0735-1097(97)00554-8.
60. **Yaniv Y, Ahmet I, Tsutsui K, Behar J, Moen JM, Okamoto Y, Guiriba TR, Liu J, Bychkov R, Lakatta EG.** Deterioration of autonomic neuronal receptor signaling and mechanisms intrinsic to heart pacemaker cells contribute to age-associated alterations in heart rate variability in vivo. *Aging Cell* 15: 716–724, 2016. doi:10.1111/acel.12483.
61. **Zimprich A, Garrett L, Deussing JM, Wotjak CT, Fuchs H, Gailus-Durner V, de Angelis MH, Wurst W, Hölter SM.** A robust and reliable non-invasive test for stress responsivity in mice. *Front Behav Neurosci* 8: 125, 2014. doi:10.3389/fnbeh.2014.00125.
62. **Zulfiqar U, Jurivich DA, Gao W, Singer DH.** Relation of high heart rate variability to healthy longevity. *Am J Cardiol* 105: 1181–1185, 2010. doi:10.1016/j.amjcard.2009.12.022.